THE ASTROPHYSICAL JOURNAL, 465:385–392, 1996 July 1

EGRET OBSERVATIONS OF HIGH-ENERGY GAMMA RADIATION FROM PSR B1706−44

D. J. THOMPSON,[1,2] M. BAILES,[3,4] D. L. BERTSCH,[2] J. A. ESPOSITO,[2,5] C. E. FICHTEL,[2] A. K. HARDING,[2] R. C. HARTMAN,[2] S. D. HUNTER,[2] R. N. MANCHESTER,[3] J. R. MATTOX,[2,6] C. VON MONTIGNY,[2,7] R. MUKHERJEE,[2,5] P. V. RAMANAMURTHY,[2,8] P. SREEKUMAR,[2,5] J. M. FIERRO,[9] Y. C. LIN,[9] P. F. MICHELSON,[9] P. L. NOLAN,[9] G. KANBACH,[10] H. A. MAYER-HASSELWANDER,[10] M. MERCK,[10] D. A. KNIFFEN,[11] E. J. SCHNEID,[12] V. M. KASPI,[13,14] S. JOHNSTON,[15] J. DAUGHERTY,[16] AND M. RUDERMAN[17]

Received 1995 October 26; accepted 1996 January 11

ABSTRACT

The Energetic Gamma-Ray Experiment Telescope (EGRET) on the *Compton Gamma Ray Observatory* has observed PSR B1706−44 a number of times between 1991 and 1995. From these data, a more detailed picture of the gamma radiation from this source has been developed, showing several characteristics that distinguish this pulsar from others: the light curve is complex, with evidence of three pulses; there is no detectable unpulsed emission; and the energy spectrum changes slope at 1 GeV. No two of the known gamma-ray pulsars have quite the same characteristics; this diversity makes interpretation in terms of theoretical models difficult.

Subject headings: gamma rays: observations — pulsars: individual (PSR B1706−44)

1. INTRODUCTION

In 1981, the second *COS B* catalog of high-energy gamma-ray sources included an entry for 2CG 342−02, an unidentified $E > 100$ MeV source near the Galactic coordinates indicated by the source name (Swanenburg et al. 1981). Nearly 10 years later, radio pulsar PSR B1706−44 was discovered during a high-frequency search of the southern sky (Johnston et al. 1992). These lines of research from opposite ends of the electromagnetic spectrum converged shortly thereafter with the identification, using data from the Energetic Gamma-Ray Experiment Telescope (EGRET) on the *Compton Gamma Ray Observatory* (*CGRO*), that the high-energy gamma radiation was pulsed at the radio period (Thompson et al. 1992).

EGRET has now detected pulsed high-energy gamma radiation from six pulsars (PSR B1706−44 and Crab, Nolan et al. 1993; Vela, Kanbach et al. 1994; PSR B1951+32, Ramanamurthy et al. 1995; Geminga, Bertsch et al. 1992, Mayer-Hasselwander et al. 1994; and PSR B1055−52, Fierro et al. 1993), with some evidence for a seventh, PSR B0656+14 (Ramanamurthy et al. 1996). Upper limits have been calculated for selected samples of radio pulsars (Thompson et al. 1994; Fierro et al. 1995) and for all cataloged pulsars (Nel et al. 1996). In particular, PSR B1509−58, which is seen at energies up to 1 MeV (Wilson et al. 1993; Matz et al. 1994; Carramiñana et al. 1995), is not detected by EGRET (Brazier et al. 1994). The present work is a detailed analysis of the EGRET observations of PSR B1706−44, based on repeated observations during 1991–1995 that have tripled the source exposure time compared with the discovery data.

The basic pulsar parameters (Taylor, Manchester, & Lyne 1993) are shown in Table 1. McAdam, Osborne, & Parkinson (1993) have suggested an association of PSR B1706−44 with a shell-type supernova remnant (SNR), G343.1−2.3. Based on distance estimates that may conflict, and on the lack of interaction of the pulsar with the remnant, Frail, Goss, & Whiteoak (1996) consider the association unlikely, though possible. They suggest instead that the pulsar lies within a small plerion seen in their 20 cm radio image. Unpulsed X-ray (Becker, Brazier, & Trümper 1995) and TeV (Kifune et al. 1995) emission have been detected from this source, although pulsations have not been reported at either of these wavelengths. As noted by Becker et al. (1995), the pulsed X-ray upper limit of 18% from *ROSAT* does not rule out a pulsed fraction similar to other pulsars observed by *ROSAT* (e.g., Vela is 11% pulsed; Ögelman, Finley, & Zimmerman 1993).

2. RADIO TIMING OBSERVATIONS

Shortly after its discovery, PSR B1706−44 was added to the list of nearly 300 pulsars that were monitored regularly by radio astronomers to assist gamma-ray telescopes on the *CGRO* (Johnston et al. 1995). High-energy gamma-ray data are sparse; weak, short-period gamma-ray pulsars are only detectable if the timing parameters are determined independently of the gamma-ray data. In the case of PSR B1706−44, this monitoring, carried out at Parkes Observatory in New South Wales, has continued. A glitch with

[1] djt@egret.gsfc.nasa.gov.
[2] Code 661, Laboratory for High-Energy Astrophysics, NASA Goddard Space Flight Center, Greenbelt, MD 20771.
[3] Australia Telescope National Facility, CSIRO, P.O. Box 76, Epping, NSW 2121, Australia.
[4] Present address: Department of Physics, University of Melbourne, Parkville, Victoria, 3052, Australia.
[5] USRA Research Associate.
[6] Compton Observatory Science Support Center, operated by USRA. Present address: Department of Astronomy, University of Maryland, College Park, MD 20742.
[7] NAS-NRC Research Associate.
[8] NAS-NRC Senior Research Associate.
[9] W. W. Hansen Experimental Physics Laboratory and Department of Physics, Stanford University, Stanford, CA 94305.
[10] Max-Planck-Institut für Extraterrestrische Physik, Giessenbachstrasse D-85748 Garching, Germany.
[11] Department of Physics, Hampden-Sydney College, Hampden-Sydney, VA 23943.
[12] Northrop Grumman Corporation, Bethpage, NY 11714.
[13] Hubble Fellow.
[14] IPAC/Caltech/JPL, Pasadena, CA 91125.
[15] Research Centre for Theoretical Astrophysics, University of Sydney, NSW 2006, Australia.
[16] Computer Science Department, University of North Carolina at Asheville, Asheville, NC 28804.
[17] Physics Department, Columbia University, New York, NY, 10027.

TABLE 1

BASIC DATA

Parameter	Value
Names	PSR B1706−44, PSR J1709−44, PSR J1709−4428
Period P	0.1024 s
Period derivative $\dot{P}$	93.0×10^{-15} s s^{-1}
Timing age τ	17,000 yr
Spin-down luminosity $\dot{E}$	3.4×10^{36} ergs s^{-1}
Magnetic field B	3.1×10^{12} G

$\delta P/P \sim 2 \times 10^{-6}$ occurred at MJD = 48775 ± 15 (Johnston et al. 1995). In addition to this glitch, the pulsar exhibits considerable timing noise. For this reason, the timing solutions used for the EGRET analysis were developed piecewise over time intervals for which the pulse phase could be adequately modeled using only a simple spin-down law. Table 2 lists the solutions relevant to the *CGRO* viewings, given in terms of frequency ν and its derivatives instead of period, and valid at time T_0. These timing solutions are from the database maintained at Princeton University (anonymous FTP: ftp://puppsr.princeton.edu/gro).

Figure 1 shows the difference between the fit and the measured radio arrival time (timing residuals) for one of these solutions. The fact that the observed radio pulse never varies from the solution by even as much as 0.2 ms is a strong indication that the gamma-ray arrival times can be converted to pulsar phase with comparable accuracy.

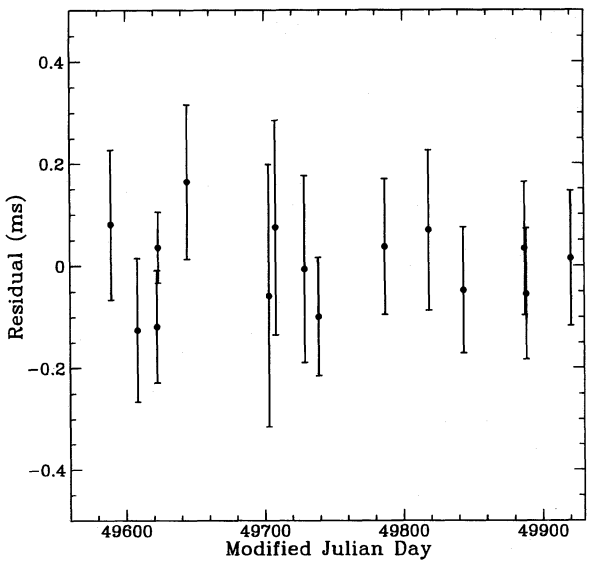

FIG. 1.—Timing residuals for PSR B1706−44. The residual is the difference between the modeled and observed radio pulse arrival time.

3. GAMMA-RAY OBSERVATIONS

EGRET, the high-energy gamma-ray telescope on the *CGRO*, is described by Thompson et al. (1993, and references therein). Operating from about 30 MeV to over 20 GeV, EGRET records individual gamma-ray photons as electron-positron pair production events. Each photon is analyzed to provide its arrival direction, its energy, and its arrival time (in Universal Coordinated Time [UTC]) to an accuracy of better than 100 μs. The field of view mapped by EGRET extends to more than 30° from the instrument axis, although the sensitivity at angles beyond 30° is less than 15% of the on-axis sensitivity. Because of the low flux level of the high-energy gamma rays, viewing intervals are typically 2–3 weeks.

PSR B1706−44 was within 30° of the telescope axis during 23 of the *CGRO* viewing intervals to date. No additional EGRET observations of this pulsar are scheduled. Table 3 is a list of the EGRET observations, showing the dates, the angle between the pulsar and the EGRET axis, and the EGRET exposure for the energy range greater than 100 MeV.

Although PSR B1706−44 is a relatively bright source compared with many others seen by EGRET (cf. the second EGRET catalog; Thompson et al. 1995), its gamma-ray count rate is nevertheless low, about two photons ($E > 100$ MeV) per hour of exposure when the source is within 10° of the EGRET axis. Data processing for EGRET relies on two principal methods: timing analysis and spatial analysis.

For the timing analysis, a set of detected photons is selected within an energy-dependent cone of radius

$$\theta \leq 5.^{\circ}85(E_\gamma/100 \text{ MeV})^{-0.534}, \quad (1)$$

with respect to the pulsar position (E_γ in MeV). This choice represents the energy-dependent angular resolution of the EGRET instrument (Thompson et al. 1993). The conversion of gamma-ray arrival time at the location of the *CGRO* to pulsar phase is carried out using a modification of the TEMPO timing program (Taylor & Weisberg 1989) and the JPL DE200 ephemeris.

TABLE 2

RADIO TIMING PARAMETERS FOR PSR B1706−44

Valid Dates	T_0 (MJD)	ν (s^{-1})	$\dot{\nu}$ (10^{-12} s^{-2})	$\ddot{\nu}$ (10^{-22} s^{-3})
1990 Jan 18–1992 May 3	48327	9.7612721442486	−8.86376	1.21
1992 Jul 9–Dec 3	48885	9.7608645998410	−8.89014	16.6
1993 Jan 13–Jul 8	49088	9.7607088316970	−8.87504	6.08
1993 Jul 19–1994 Dec 22	49447	9.7604336985587	−8.86669	2.19
1994 Aug 25–1995 Jul 22	49754	9.7601985856255	−8.86125	1.97

TABLE 3

EGRET OBSERVATIONS OF PSR B1706−44

Viewing Number	Observation Dates	Aspect Angle	Exposure (>100 MeV) (10^7 cm^2 s)
0050	1991 Jul 12–26	16°.9	25.9
0160	1991 Dec 12–27	28.3	10.8
0230	1992 Mar 19–Apr 2	21.7	5.7
0270	1992 Apr 28–May 7	12.0	9.7
0350	1992 Aug 6–11	24.1	1.9
0380	1992 Aug 27–Sep 1	24.1	3.0
2100	1993 Feb 22–25	15.4	2.3
2140	1993 Mar 29–Apr 1	15.4	3.1
2190	1993 May 5–8	19.8	0.9
2230	1993 May 31–Jun 3	16.2	3.0
2260	1993 Jun 19–29	14.2	10.5
2290	1993 Aug 10–11	23.2	0.5
2295	1993 Aug 12–17	23.2	2.6
2320	1993 Aug 24–Sep 7	5.2	19.0
3023	1993 Sep 9–21	21.8	5.8
3230	1994 Mar 22–Apr 5	16.1	16.2
3340	1994 Jul 18–25	26.4	3.3
3365	1994 Aug 4–9	6.2	7.7
4210	1995 Jun 6–13	12.6	8.8
4220	1995 Jun 13–20	12.5	11.2
4230	1995 Jun 20–30	19.6	10.6
4235	1995 Jun 30–Jul 10	16.4	11.3

The spatial analysis compares the observed gamma-ray map with that expected from a model of the diffuse Galactic and extragalactic radiation (Hunter et al. 1996). Source location and flux as a function of energy are determined using a maximum likelihood method (Mattox et al. 1996). The timing and spatial approaches can also be combined to produce phase-resolved maps and energy spectra.

4. RESULTS

4.1. *Light Curve*

Compared with the very bright Crab, Vela, and Geminga gamma-ray pulsars (Ramanamurthy et al. 1995), PSR B1706−44 is considerably weaker and lies in the Galactic center region where the diffuse Galactic gamma radiation is much more intense. For these reasons, the results are characterized by somewhat larger uncertainties than seen for these other pulsars.

Figure 2 shows the light curve for PSR B1706−44 for energies above 400 MeV, including all viewing periods listed in Table 3. The peak of the single radio pulse (Johnston et al. 1992) defines phase 0 on this 50 bin plot. The gamma-ray energy selection is based on maximizing the significance of the pulsed signal, as characterized by the (binned) χ^2 or (unbinned) H-test value (de Jager, Swanepoel, & Raubenheimer 1978). For lower energies, the larger acceptance cone introduces more Galactic background, while the statistics are reduced for higher energies.

The gamma-ray light curve, which for this selection contains 1325 gamma rays, is more complex than those of the Crab, Vela, Geminga, and PSR B1951+32, all of which show two narrow peaks separated by 0.4–0.5 in phase. In the case of Vela, for example, the pulse widths (FWHM) are a few milliseconds (Kanbach et al. 1994). PSR B1055−52 (Fierro et al. 1993) has what appears to be a single broad pulse in gamma rays, but the statistics for this pulsar are far smaller than those for PSR B1706−44. Between phases 0.2 and 0.6, PSR B1706−44 shows at least two, and possibly three, peaks. Figure 3 shows the same data plotted in 100 bins (and explicitly displaying the uncertainties due to counting statistics) with three possible fits to the pulse shape: (1) a fit consisting of a single Gaussian peak plus a constant background ($\chi^2 = 139$ for 96 degrees of freedom [dof] [100 bins minus 4 degrees of constraint for the fit], with probability = 0.007 for this χ^2); (2) a fit using two Gaussians plus a constant ($\chi^2 = 99$ for 93 dof, probability = 0.32); and (3) a fit with three Gaussians plus a constant ($\chi^2 = 90$ for 90 dof, probability = 0.48). Although the fit using a single peak can be rejected with high confidence, the difference between the two Gaussian and three Gaussian fit is not compelling. An F-test indicates that the two Gaussian plus constant fit has a 60% probability of being acceptable. Nevertheless, the third (middle) peak appears to be a persistent feature, appearing consistently when the data set is divided in half by time (Fierro 1995). Based on these fits, the two principal peaks in the light curve fall at phases 0.27 ± 0.02 and 0.45 ± 0.02 and have FWHM of approximately 12 ms each. The third peak, if included, falls at phase 0.36 ± 0.02 and has FWHM = 3 ms.

Figure 4 shows the light curve in four energy bands. The decrease in background and the decrease in statistics with increasing energy are both clear from this figure. Above 5 GeV, all 12 photons fall into the pulse region. The basic

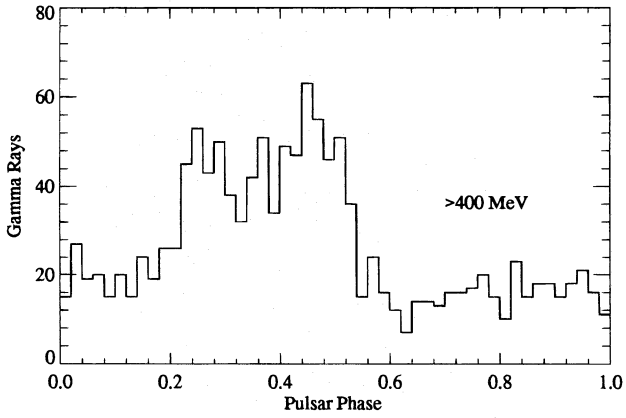

FIG. 2.—High-energy gamma-ray light curve for PSR B1706−44. The 102 ms period is divided into 50 phase bins. The single radio pulse defines the zero phase.

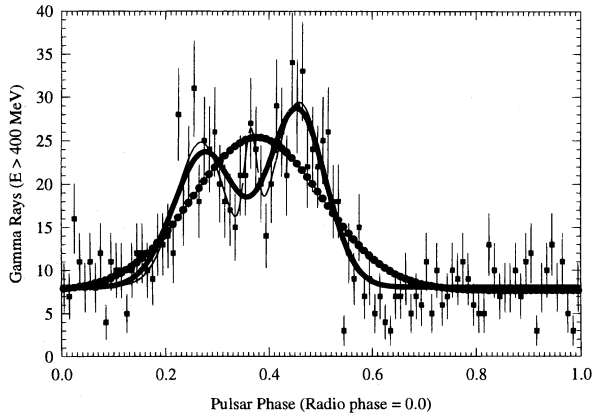

FIG. 3.—High-energy gamma-ray light curve for PSR B1706−44, with 100 phase bins. Uncertainties due to counting statistics are shown. The fitted curves, as described in the text, are two Gaussian peaks plus a constant background (*heavy solid line*), three Gaussian peaks plus a constant background (*light solid line*), and single Gaussian peak plus a constant background (*heavy dotted line*).

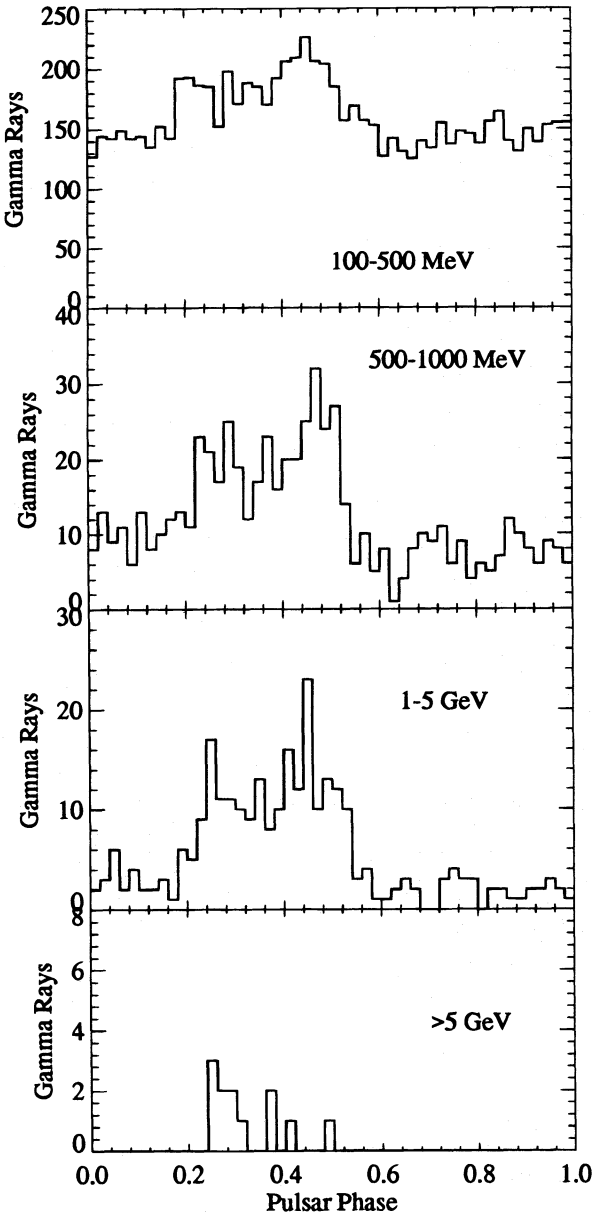

FIG. 4.—Gamma-ray light curve for PSR B1706−44 in four energy ranges, with 50 bin resolution.

structure of the light curve is similar at all energies, with strong indications of two peaks and some evidence of three peaks seen at all energies. The evidence of pulsed emission extends well above 5 GeV, in contrast to Geminga and Vela, which show strong cutoffs above a few GeV. Of the 12 highest energy photons, five have measured energies above 10 GeV, and one has a measured energy of 64 ± 34 GeV.

From 30 to 100 MeV, the pulsed signal is harder to separate from the surrounding Galactic background. The signal is still visible, however, if a narrower cone is taken rather than the one described above. The EGRET point-spread function itself has a narrow and a broad component (Thompson et al. 1993), and by selecting a narrower range, specifically a fixed cone of half-angle 2°.5, it is possible to obtain a light curve whose probability of occurring by chance is less than 10^{-5}. The pulse shape is consistent with that seen at the higher energies.

4.2. *Search for Unpulsed Emission and Time History of Total Emission*

Although Figure 4 makes it clear that the gamma radiation from PSR B1706−44 is strongly dominated by the pulsed emission at high energies, a search for unpulsed emission can be undertaken over broader energy ranges. In the region of sky mapped by EGRET around the pulsar, each photon's arrival time is converted to pulsar phase, whether or not this photon is likely to have come from the pulsar itself. Phase-resolved maps of the sky are then constructed, and the spatial analysis using maximum likelihood (Mattox et al. 1996) is used to assess the statistical significance of a source at the pulsar location. The likelihood ratio test is used to determine the significance of point sources. The likelihood ratio test statistic is $TS \equiv 2(\ln L_1 - \ln L_0)$, where $\ln L_1$ is the log of the likelihood of the data if a point source is included in the model, and $\ln L_0$ is the log of the likelihood of the data without a point source. For positive values of TS, the analysis gives the most likely gamma-ray flux of a source at the pulsar location. The result in each phase bin for $E > 100$ MeV is shown in Figure 5. The pulsar is detected with high significance only between phases 0.2 and 0.55, exactly the range expected from the light curves. There is weaker evidence for a leading wing and a trailing wing, but no evidence for a source in the rest of the phases. Table 4 shows the results of the phase-resolved analysis for two broad energy ranges. In each case, the flux is time averaged over the entire phase. In the absence of any unpulsed emission, the pulsed flux is equivalent to the total flux. Above 100 MeV, the unpulsed component is less than 20% of the pulsed (total) emission.

Figure 6 shows the $E > 100$ MeV EGRET observations of PSR B1706−44 flux as a function of time, from 1991 to

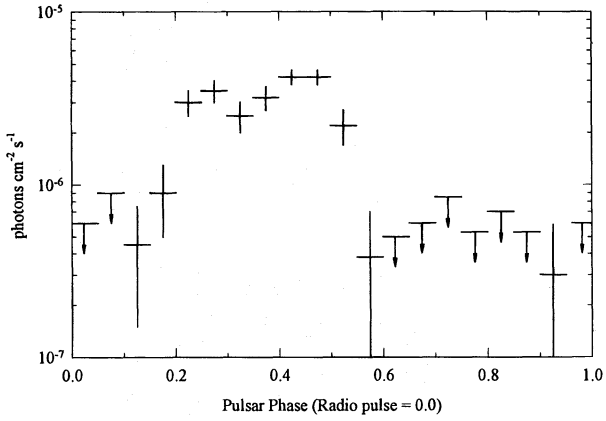

FIG. 5.—$E > 100$ MeV gamma-ray flux at the location of PSR B1706−44 as a function of pulsar phase.

TABLE 4

PULSED AND UNPULSED RESULTS

Energy Range	Pulsed Flux	Unpulsed Limit (95% confidence)
$30 < E < 100$ MeV.....	$1.05 \pm 0.24 \times 10^{-6}$	$<1.01 \times 10^{-6}$
$E > 100$ MeV.....	$1.28 \pm 0.08 \times 10^{-6}$	$<0.24 \times 10^{-6}$

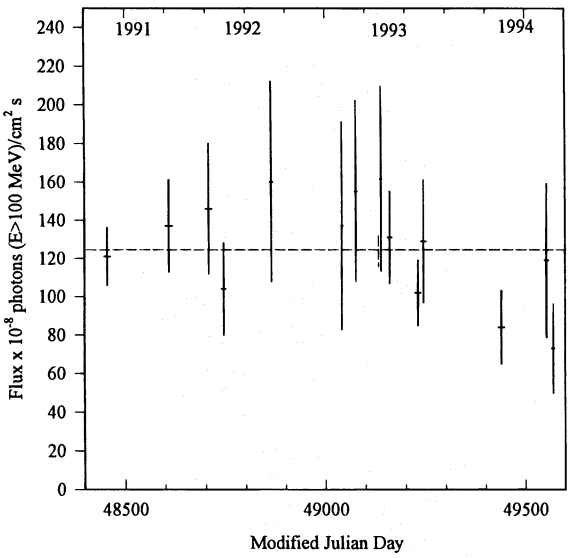

FIG. 6.—$E > 100$ MeV gamma-ray flux at the location of PSR B1706−44 as a function of time. Each data point represents one viewing period. The uncertainties shown are statistical only.

1994. The 1995 observations were affected by known drifts in the EGRET performance due to the deterioration of the spark chamber gas and have therefore been excluded. The dashed line is the flux calculated from the summed exposure to the pulsar. As for the Crab, Geminga, and Vela pulsars (Ramanamurthy et al. 1995), the gamma radiation from PSR B1706−44 appears to be steady. The χ^2 is 13 for 13 dof.

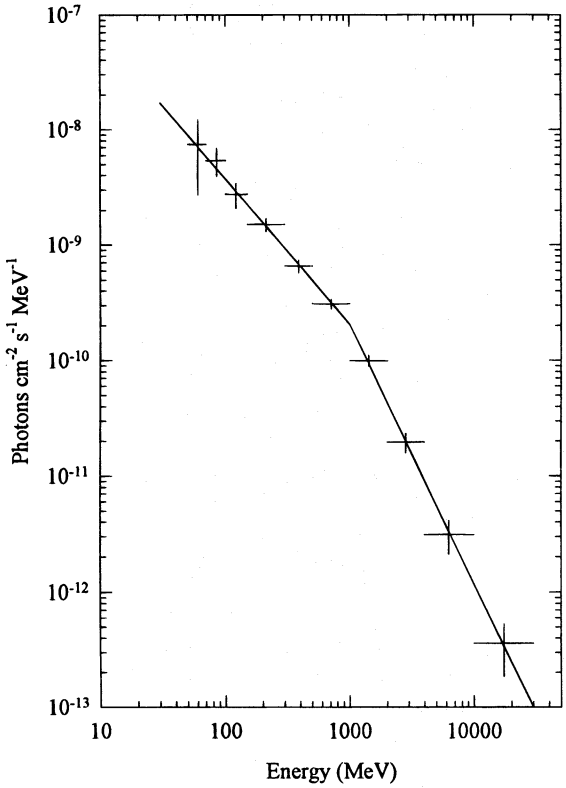

FIG. 7.—Phase-averaged energy spectrum of PSR B1706−44. The fit to a broken power law is described in the text. The uncertainties shown are statistical only.

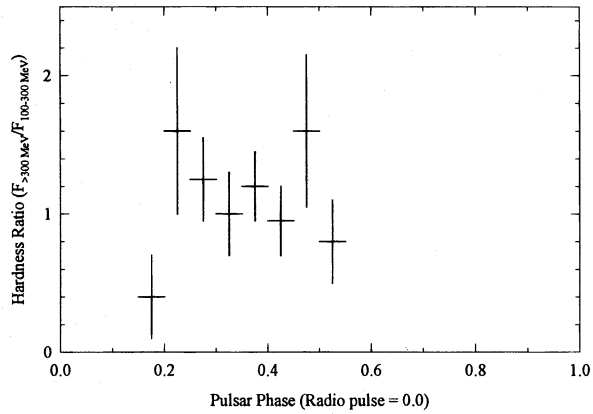

FIG. 8.—Hardness ratio (flux for $E > 300$ MeV/flux for 100–300 MeV) of PSR B1706−44 as a function of pulsar phase.

4.3. *Energy Spectrum*

Because there is no evidence for unpulsed emission, the energy spectrum of the pulsar can be derived by defining the background level in any energy band as the flux seen in the off-pulse part of the light curve. The excesses in each band are then compared with model spectra forward folded through the EGRET energy response function, as described by Nolan et al. (1993). Pulsed emission is detected from 50 MeV to more than 10 GeV. The spectrum, shown in Figure 7 as a phase-averaged photon number spectrum, is well described by a broken power law,

$$\frac{dN}{dE} = (2.05 \pm 0.19) \times 10^{-10}\left(\frac{E}{1000\ \text{eV}}\right)^{\alpha} \text{photons cm}^{-2}\ \text{s}^{-1}\ \text{MeV}^{-1}\,, \quad (2)$$

where

$$\alpha = \begin{cases} -1.27 \pm 0.09 & E \le 1000\ \text{MeV}\,, \\ -2.25 \pm 0.13 & E \ge 1000\ \text{MeV}\,. \end{cases} \quad (3)$$

The Crab, Vela, and Geminga pulsars all show spectral variations as a function of pulsar phase in the EGRET energy range. Although PSR B1706−44 is weaker than these three, the possibility of spectral variation can be examined. Figure 8 shows the hardness ratio, the flux above 300 MeV divided by the flux from 100 to 300 MeV, for PSR B1706−44 as a function of phase, using the same 20 phase bins as in Figure 4. With the possible exception of the leading wing of the pulse (phase 0.15–0.20), the hardness ratio is consistent for all the pulsed emission. Energy spectra constructed for portions of the phase corresponding to the peaks are also consistent with each other (Fierro 1995).

5. DISCUSSION

5.1. *Light Curves*

The overall gamma-ray light curve for PSR B1706−44 differs markedly from those of most of the other gamma-ray

pulsars. The Crab, Vela, Geminga, and PSR B1951+32 light curves are all chracterized by two narrow pulses separated by 0.4–0.5 in phase. PSR B1509−58 (seen only $\lesssim$1 MeV) has a well-defined single pulse, and PSR B1055−52 has a broad single pulse (although not well defined due to limited statistics). PSR B1706−44 shows two broader pulses with a phase separation of 0.2. This distinction points strongly to a different beaming geometry for this pulsar than for the others. Radio polarization studies, for example, indicate that PSR B1706−44 has its rotation and magnetic axes more aligned than Vela (Guojun et al. 1995). The possible third peak in the light curve is unique to PSR B1706−44 among gamma-ray pulsars. In this respect, it resembles radio pulsar light curves that have both core and conal emissions (e.g., Rankin 1991).

5.2. *Distance*

The distance determined from the dispersion measure (DM) 75.69 cm^{-3} pc (Taylor & Cordes 1993) is 1.8 (−0.5, +0.7) kpc. Kinematic distance limits derived from H I absorption (Koribalski et al. 1995) are $D_{\rm Lower} = 2.4 \pm 0.6$ kpc and $D_{\rm Upper} = 3.2 \pm 0.4$ kpc. The possible association of PSR B1706−44 with the SNR G343.1−2.3 (McAdam et al. 1993) would imply a distance of 3 kpc based on the Σ-D relation. For purposes of calculation, we adopt a distance of 2.4 kpc, consistent with both the DM and H I measurements. It is important to recognize that all such distance estimates have uncertainties of 25% or more.

5.3. *Luminosity and Beaming*

In terms of the observed energy flux F_E, the gamma-ray luminosity of a pulsar is

$$L_\gamma = 4\pi f F_E D^2 , \quad (4)$$

where f is the fraction of the sky into which the pulsar radiates and D is the distance to the pulsar. This beaming fraction f is highly uncertain. Based on the pulse shape, Thompson et al. (1992) used a value of 0.27. In a nearly aligned rotator model, Dermer & Sturner (1994) find a beaming fraction of less than 0.1, while an outer-gap model (Yadigaroglu & Romani 1995) suggests a value of 0.55. In comparing the EGRET-detected pulsars, Thompson et al. (1994) adopted a value of $1/4\pi$.

The observed energy flux obtained by integrating equation (2) in the range 100 MeV–10 GeV is $(9.4 \pm 1.2) \times 10^{-10}$ ergs cm^{-2} s. For a distance of 2.4 kpc, the gamma-ray luminosity of PSR B1706−44 is then $(5 \pm 3) \times 10^{34} \times 4\pi f$ ergs s^{-1}. Unless the beaming fraction is extremely small, the gamma radiation represents on the order of 1% of the spin-down luminosity, $\dot{E} = 3.4 \times 10^{36}$ ergs s^{-1}.

5.4. *Broadband Energy Spectrum*

The multiwavelength spectrum of PSR B1706−44 is shown in Figure 9, using two different formats. At the top, the photon number spectrum is shown. The photon spectrum falls steadily across the entire electromagnetic spectrum. At the bottom, the frequency versus νF_ν display shows the observed power per log (frequency). Pulsed emission is detected from PSR B1706−44 only in the radio and high-energy gamma-ray bands. Unpulsed emission, which is associated with the pulsar on the basis of positional information, is seen in the *ROSAT* X-ray range (Becker et al. 1995) and in the very high energy gamma-ray regime using ground-based detection of the Cerenkov radiation from gamma-ray–induced particles (Kifune et al. 1995). Because of the very flat energy spectrum below 1 GeV, the OSSE (Schroeder et al. 1995) and COMPTEL (Carramiñana et al. 1995) observations yield only upper limits. EGRET obtains positive detections from 50 MeV to about 20 GeV. The maximum νF_ν occurs near 1 GeV, the break in the observed EGRET spectrum. The observable power from this pulsar is strongly dominated by the gamma-ray emission.

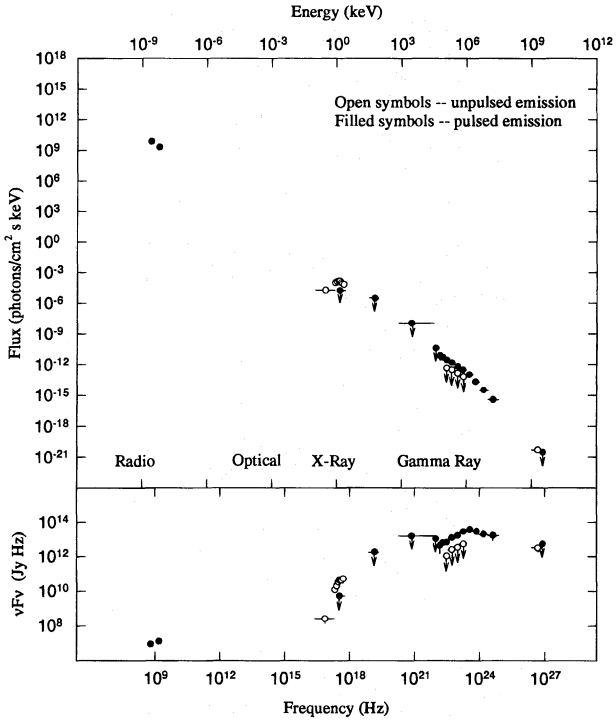

FIG. 9.—Multiwavelength spectrum of PSR B1706−44. *Top*, photon number spectrum; *bottom*, the frequency ν vs. νF_ν. References are radio (Taylor et al. 1993; Johnston et al. 1992); X-ray (*ROSAT*), the 2 σ pulsed upper limit is 18% of the unpulsed emission (Becker et al. 1995); gamma ray, OSSE (Schroeder et al. 1995) and COMPTEL (Carramiñana et al. 1995); EGRET (present results); TeV detection (unpulsed) (Kifune et al. 1995); and TeV pulsed upper limit (Nel et al. 1994).

5.5. *Gamma-Ray Pulsar Models*

Two general classes of models have been proposed for gamma-ray pulsars. In polar cap models (recent examples are Daugherty & Harding 1994, 1996 and Sturner & Dermer 1995), the particle acceleration and gamma-ray production takes place in the open field line region above the magnetic pole of the neutron star. In outer gap models (recent examples are Ho 1993 and Romani & Yadigaroglu 1995), the interaction region lies in the outer magnetosphere in vacuum gaps associated with the last open field line. In either of these models, PSR B1706−44 could be expected to be a detectable gamma-ray pulsar, because its physical parameters are quite similar to those of Vela. The details of the gamma-ray observations, however, are not all readily explained by either model.

Because either type of model can be viewed as having a hollow cone geometry, a double pulse has a straightforward

explanation. The observer's line of sight cuts across the edge of the cone at two places. Although the specific details depend on the size of the beam, and its relationship to the rotation axis and the observer's line of sight, in the case of PSR B1706−44, one possibility is that the line of sight is closer to the edge of the cone than for the pulsars with two widely spaced light-curve peaks. The fact that the peaks are broader for PSR B1706−44 is also consistent with this geometric picture, because the line of sight crosses the cone at a shallower angle.

Following from the geometric picture, the existence of a third pulse is not expected in the simplest version of either model. An earlier version of the outer gap model (Cheng, Ho, & Ruderman 1986) predicted that gamma-ray pulsars could have up to four peaks, with the second pair of peaks arising from particle beams moving inward as well as outward along the outer gap. More recent outer gap models expect much less radiation from the inward-moving beams (Chiang & Romani 1994). A unified polar cap/outer gap model (Kamae & Sekimoto 1995) can explain three peaks in the light curve, but this model predicts that the middle peak should be broad and have a soft spectrum, in contrast to the present observations. In the absence of any evidence for a third pulse in the other gamma-ray pulsars, PSR B1706−44 appears to be distinctive in this respect.

The energy spectrum presents similar challenges. In the polar cap models, a sharp turnover is expected in the few to 10 GeV energy range due to attenuation of the gamma-ray flux in the magnetic field (Daugherty & Harding 1994, 1996). The spectral change in the 1 GeV range does not appear to fit this model, although there could be a sharp break in the energy range above 20 GeV, as suggested by the absence of pulsed TeV emission. On the other hand, the lack of variation of the spectrum with pulsar phase for PSR B1706−44 is expected in the Daugherty & Harding (1996) polar cap model. The outer gap model does predict a flattening of pulsar spectra at lower energies (Ho 1993), although, in the case of Vela, this flattening occurs well below 100 MeV, not near 1 GeV, and the flattening is to an $E^{-0.67}$ spectrum, not $E^{-1.27}$ as observed. The dependence of the spectrum on the geometry has not been extensively studied in the outer gap model. It is fair to say that the spectral shape of PSR B1706−44 was not predicted by any model.

A reasonable hypothesis is that the difference in the beaming/observer geometry (compared with the brighter gamma-ray pulsars), which produces the unusual pulse shape for PSR B1706−44, is also responsible for the different energy spectrum. How these observed features relate to the gamma-ray production process is unclear. PSR B1055−52 is the pulsar closest to PSR B1706−44 in light-curve shape; therefore, its energy spectrum might show a similar feature. Unfortunately, the statistics for both the light curve and the energy spectrum of PSR B1055−52 are much more limited (Fierro et al. 1993) and cannot at present address this question.

6. SUMMARY

PSR B1706−44 is one of at least six spin-powered pulsars seen at gamma-ray energies above 100 MeV. Observations from EGRET on the *CGRO* between 1991 and 1995 have provided new details of the gamma radiation:

1. The light curve is complex, with at least two peaks separated by about 0.2 in phase, with some evidence of a third peak. None of the other gamma-ray pulsars show a similar light curve.
2. There is no detectable unpulsed gamma radiation from the pulsar.
3. There is no evidence that the gamma-ray flux from the pulsar varies on long timescales.
4. The gamma-ray energy spectrum can be represented by a broken power law, with a break near 1 GeV. The spectral index changes by 1.0, in contrast to the Vela and Geminga spectra, which have sharp spectral breaks (index change greater than 1) in the few GeV energy range.
5. The maximum observable power from the pulsar is in the gamma-ray energy range. The observed X-ray emission is unpulsed, with a pulsed fraction less than 18%. The TeV emission is also not pulsed. The Crab is the only other pulsar seen at TeV energies, and its TeV emission is not pulsed.
6. The gamma radiation represents about 1% of the spin-down luminosity of the pulsar, although the unknown beaming geometry makes this estimate uncertain.
7. Present gamma-ray pulsar models offer no straightforward explanation of either the light-curve shape or the energy spectrum.

The EGRET team gratefully acknowledges support from the following: Bundesministerium für Forschung und Technologie, grant 50 QV 9095 (MPE authors); NASA grant NAG5-1742 (HSC); NASA grant NAG5-1605 (SU); and NASA contract NAS5-31210 (GAC).

Parts of this work were carried out by one of the authors (J. M. F.) in partial fulfillment of the doctor of philosophy requirements for Stanford University.

V. M. K. thanks NASA for support via a Hubble Fellowship through grant HF-1061.01-94A from the Space Telescope Science Institute, which is operated by the Association of Universities for Research in Astronomy, Inc., under NASA contract NAS5-26555. Part of this research was carried out at the Jet Propulsion Laboratory, California Institute of Technology, under contract with NASA.

J. R. M. acknowledges support from NASA grant NAG5-2833.

REFERENCES

Becker, W., Brazier, K. T. S., & Trümper, J. 1995, A&A, 298, 528
Bertsch, D. L., et al. 1992, Nature, 357, 306
Brazier, K. T. S., et al. 1994, MNRAS, 268, 517
Carramiñana, A., et al. 1995, A&A, 304, 258
Cheng, K. S., Ho, C., & Ruderman, M. 1986, ApJ, 300, 522
Chiang, J., & Romani, R. W. 1994, ApJ, 436, 754
Daugherty, J. K., & Harding, A. K. 1994, ApJ, 429, 325
———. 1996, ApJ, 458, 278
De Jager, O. C., Swanepoel, J. W. H., & Raubenheimer, B. C. 1978, A&A, 221, 180
Dermer, C. D., & Sturner, S. J. 1994, ApJ, 420, L75
Fierro, J.M. 1995, Ph.D. thesis, Stanford Univ.
Fierro, J.M., et al. 1993, ApJ, 413, L27
———. 1995, ApJ, 447, 807
Frail, D. A., Goss, W. M., & Whiteoak, J. B. Z. 1996, ApJ, submitted
Guojun, Q., Manchester, R. N., Lyne, A. G, & Gould, D. M. 1995, MNRAS, 274, 572
Ho, C. 1993, in Isolated Pulsars, ed. K. A. Van Riper, R. Epstein, & C. Ho (Cambridge: Cambridge Univ. Press), 271
Hunter, S. D., et al. 1996, ApJ, in press
Johnston, S., Lyne, A. G., Manchester, R. N., Kniffen, D. A., D'Amico, N., Lim, J., & Ashworth, M. 1992, MNRAS, 255, 401
Johnston, S., Manchester, R. M., Lyne, A. G., Kaspi, V. M., & D'Amico, N. 1995, A&A, 293, 795

Kamae, T., & Sekimoto, Y. 1995, ApJ, 443, 780
Kanbach, G., et al. 1994, A&A, 289, 855
Kifune, T., et al. 1995, ApJ, 438, L91
Koribalski, B., Johnston, S., Weisberg, J. M., & Wilson, W. 1995, ApJ, 441, 756
Mattox, J. R., et al. 1996, ApJ, 461, 396
Matz, S. M., et al. 1994, ApJ, 434, 288
Mayer-Hasselwander, H. A., et al. 1994, ApJ, 421, 276
McAdam, W. B., Osborne, J. L., & Parkinson, M. L. 1993 Nature, 361, 516
Nel, H. I., De Jager, O. C., Raubenheimer, B. C., Brink, C., Meintjes, P. J., & North, A. R. 1993, ApJ, 418, 836
Nel, H. I., et al. 1996, ApJ, in press
Nolan, P. L., et al. 1993, ApJ, 409, 697
Ögelman, H., Finley, J. P., & Zimmerman, H. U. 1993, Nature, 361, 136
Ramanamurthy, P. V., et al. 1995, ApJ, 447, L109
Ramanamurthy, P. V., Fichtel, C. E., Kniffen, D. A., Sreekumar, P., & Thompson, D. J. 1996, ApJ, 458, 755
Rankin, J. M. 1991, Ann. NY Acad. Sci., 647, 519
Romani, R. W., & Yadigaroglu, I.-A. 1995, ApJ, 438, 314
Schroeder, P. C., et al. 1995, ApJ, 450, 784
Sturner, S. J., & Dermer, C. D. 1994, ApJ, 420, L79
Swanenburg, B. N., et al. 1981, ApJ, 243, L69
Taylor, J. H., & Cordes, J. M. 1993, ApJ, 411, 674
Taylor, J. H., Manchester, R. N., & Lyne, A. G. 1993, ApJS, 88, 529
Taylor, J. H., & Weisberg, J. M. 1989, ApJ, 345, 434
Thompson, D. J., et al. 1992, Nature, 359, 615
———. 1993, ApJS, 86, 629
———. 1994, ApJ, 436, 229
———. 1995, ApJS, 101, 259
Wilson, R. B., Finger, M. H., Pendelton, G. N., Fishman, G. J., Meegan, C. A., & Paciesas, W. S. 1993, in Isolated Pulsars, ed. K. A. Van Riper, R. Epstein, & C. Ho (Cambridge: Cambridge Univ. Press), 257
Yadigaroglu, I.-A., & Romani, R. W. 1995, ApJ, 449, 211